

Valley-Coherent Quantum Anomalous Hall State in AB-Stacked MoTe₂/WSe₂ BilayersZui Tao,^{1,‡} Bowen Shen,^{1,‡} Shengwei Jiang,^{2,‡} Tingxin Li,^{1,‡} Lizhong Li,¹ Ligu Ma,¹ Wenjin Zhao^{ⓧ,3}, Jenny Hu,⁴ Kateryna Pistunova,⁴ Kenji Watanabe,⁵ Takashi Taniguchi,⁵ Tony F. Heinz,^{4,6} Kin Fai Mak^{ⓧ,1,2,3,*} and Jie Shan^{1,2,3,†}¹School of Applied and Engineering Physics, Cornell University, Ithaca, New York, USA²Laboratory of Atomic and Solid State Physics, Cornell University, Ithaca, New York, USA³Kavli Institute at Cornell for Nanoscale Science, Ithaca, New York, USA⁴Departments of Physics and Applied Physics, Stanford University, Stanford, California, USA⁵National Institute for Materials Science, 1-1 Namiki, 305-0044 Tsukuba, Japan⁶SLAC National Accelerator Laboratory, Menlo Park, California, USA

(Received 11 June 2023; revised 18 September 2023; accepted 8 December 2023; published 10 January 2024)

Moiré materials provide fertile ground for the correlated and topological quantum phenomena. Among them, the quantum anomalous Hall (QAH) effect, in which the Hall resistance is quantized even under zero magnetic field, is a direct manifestation of the intrinsic topological properties of a material and an appealing attribute for low-power electronics applications. The QAH effect has been observed in both graphene and transition metal dichalcogenide (TMD) moiré materials. It is thought to arise from the interaction-driven valley polarization of the narrow moiré bands. Here, we show that the newly discovered QAH state in AB-stacked MoTe₂/WSe₂ moiré bilayers is not valley polarized but valley coherent. The layer- and helicity-resolved optical spectroscopy measurement reveals that the QAH ground state possesses spontaneous spin (valley) polarization aligned (antialigned) in two TMD layers. In addition, saturation of the out-of-plane spin polarization in both layers occurs only under high magnetic fields, supporting a canted spin texture. Our results call for a new mechanism for the QAH effect and highlight the potential of TMD moiré materials with strong electronic correlations and spin-orbit interactions for exotic topological states.

DOI: 10.1103/PhysRevX.14.011004

Subject Areas: Condensed Matter Physics, Magnetism, Strongly Correlated Materials

I. INTRODUCTION

Narrow bands with nontrivial topology are believed to be the key to realizing interaction-driven topological states [1–3]. Moiré superlattices formed in Van der Waals bilayers with a small twist angle or lattice mismatch can induce narrow moiré bands [1,4–6]. These narrow bands enhance the importance of electronic correlations, as manifested in the emergence of superconductivity [4,7] and a set of correlated insulating states in graphene and transition metal dichalcogenide (TMD) moiré materials [1,4–6]. Topological states have also been proposed in these materials based on valley contrast physics; that is, moiré bands possess opposite Chern numbers in the K and K' valleys of the Brillouin zone [1,2,8–13]. In particular,

the quantum anomalous Hall (QAH) effect [14–16] has been observed in graphene-based moiré systems [17–22], and is consistent with a fully valley-polarized ground state as a result of the interaction-driven valley symmetry breaking [1,2,8,10–13]. A similar mechanism has been put forward for AA-stacked (near-0°-aligned) TMD homobilayers such as MoTe₂ and WSe₂ [9,23]. Unlike graphene, TMD monolayers have broken inversion symmetry, and possess strong Ising spin-orbit interactions and spin-valley locking [24,25]. Because of the large spin splitting at the monolayer valence band maximum, the low-energy valence states of the bilayer at the K (or K') valley can be described by two bands, one from each layer. Valley Chern bands with opposite Chern numbers can form from a topologically nontrivial interlayer tunneling structure that has the moiré period [9,23]. A topological Kane-Mele model is realized with the Wannier orbitals of the two layers forming a honeycomb lattice.

Recently, the QAH effect was observed in AB-stacked (near-60°-aligned) MoTe₂/WSe₂ moiré bilayers [26]. In the absence of an out-of-plane electric field E , the bands (about 10 meV bandwidth) are expected to be topologically trivial [27,28]; the system is a Mott insulator with one hole per moiré unit cell that resides in the MoTe₂ layer and the MM site ($M = \text{Mo}, \text{W}$) [Fig. 1(a)]. A large electric field

*Corresponding author: kinfai.mak@cornell.edu

†Corresponding author: jie.shan@cornell.edu

‡These authors contributed equally to this work.

Published by the American Physical Society under the terms of the [Creative Commons Attribution 4.0 International license](https://creativecommons.org/licenses/by/4.0/). Further distribution of this work must maintain attribution to the author(s) and the published article's title, journal citation, and DOI.

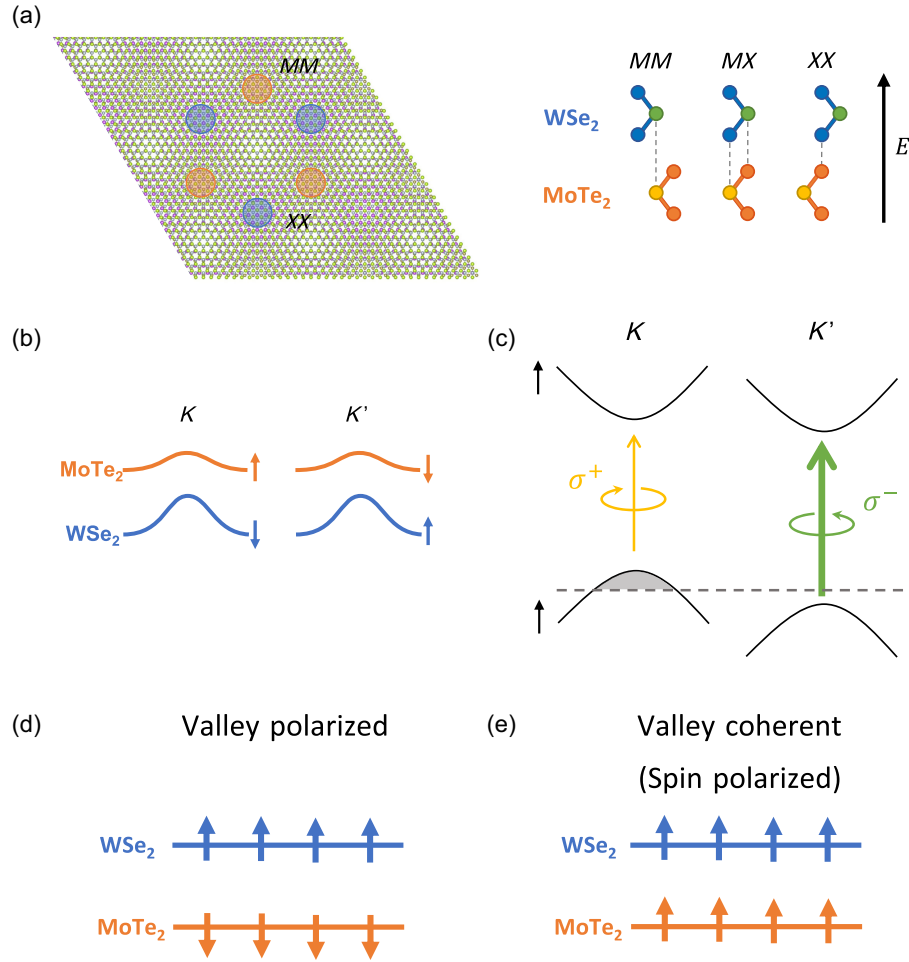


FIG. 1. AB-stacked MoTe₂/WSe₂ moiré bilayers. (a) moiré pattern (left) formed in 60°-aligned (or antiparallel) MoTe₂ and WSe₂ bilayers (right). *MM*, *MX*, and *XX* ($M = \text{Mo, W}$; $X = \text{Se, Te}$) are the high-symmetry stacking sites. The Wannier orbital of the two layers occupies the *MM* and *XX* sites, forming a honeycomb lattice. An out-of-plane electric field (E) from MoTe₂ to WSe₂ induces the QAH effect. (b) Schematics of the topmost valence bands at the K and K' valley from two layers. Arrows denote the out-of-plane spin alignment. In each layer, spin and valley are locked. In each valley, two bands have opposite spins. (c) Optical selection rules in monolayer TMDs. Attractive polaron, a bound state of the electron-hole excitation in the K (K') valley and hole excitations in the K' (K) valley, couples exclusively to the σ^+ (σ^-) excitation. When the holes occupy K valley only, the σ^- excitation dominates. The dashed line denotes the Fermi level. (d),(e) Two possible QAH ground states: valley polarized (d) and valley coherent (or spin polarized) (e), in which the spin polarization is antialigned and aligned in two layers, respectively.

reduces the band offset between the two layers, inverts the bands, and drives a topological phase transition to a QAH insulator (also referred to as Chern insulator); this is also accompanied by a partial transfer of the holes to the WSe₂ layer and the *XX* site ($X = \text{Se, Te}$). The experimental result is quite surprising: although AB-stacked MoTe₂/WSe₂ moiré bilayers can be described by a two-band model on a honeycomb lattice [27,28] as in the case of AA-stacked TMD moiré homobilayers [9,23] [Fig. 1(a)], the two bands have opposite spins, and interlayer tunneling is nearly spin forbidden [Fig. 1(b)]; i.e., the two TMD layers are largely decoupled. A variety of theories have been proposed to explain the experimental result [27–35]. It was pointed out that valley Chern bands could still form from a strain pseudo-magnetic field [29] or from a weak interlayer

tunneling when the out-of-plane spin is no longer strictly conserved [27]; both can be induced by lattice reconstruction in moiré bilayers. These theories naturally predict a (fully or partially) valley-polarized QAH ground state [27–32,35].

In this study, we directly probe the magnetic properties of the QAH state in AB-stacked MoTe₂/WSe₂ moiré bilayers by layer-resolved and helicity-resolved spectroscopy. We show that the holes are distributed in both layers, and the QAH ground state is valley coherent [or spin polarized, Fig. 1(e)], i.e., hybridization of states from different valleys near the Fermi level, thus opening a correlated charge gap. This is in contrast to the theoretical predictions [27–32,35] of a valley-polarized [Fig. 1(d)] QAH ground state, i.e., hybridization of states from different

layers of the same valley. Theoretical studies beyond the current frame of noninteracting valley states may be required to understand the experimental results [33,34].

II. OPTICAL SELECTION RULES

The current measurement relies on the unique optical selection rules for intralayer excitations in TMDs [24,25] [Fig. 1(c)]. In the presence of doping, the optical excitations are dominated by polarons (or charged excitons) instead of neutral excitons [36,37]; particularly, the attractive polaron is a bound state of a photoexcited exciton in one valley and charge excitations in the other valley due to the Pauli exclusion principle. The attractive polaron with exciton in the K (K') valley is exclusively coupled to the left (right) circularly polarized light, σ^+ (σ^-), in the MoTe₂ layer. Magnetic circular dichroism (MCD) emerges when the layer is spin or valley polarized. In the extreme case of doped holes occupying only one spin-valley state, the attractive polaron response vanishes for one of the helicities [25,36,38]. Furthermore, because of the AB-stacking structure, the optical selection rules in the WSe₂ layer are reversed (identical) for valley (spin). Hence, if the attractive polaron response in two layers is dominated by excitation of opposite helicities, the holes occupy opposite spin states, and the bilayer is valley polarized [Fig. 1(d)]. Conversely, if the response is dominated by identical helicities, the holes occupy same spin states, and the bilayer is in a superposition of two valley states [Fig. 1(e)]. The optical selections have been independently verified in separate MoTe₂ and WSe₂ monolayers polarized by a large out-of-plane magnetic field (Supplemental Material, Fig. 1 [39]). The selection rules are expected to be valid in AB-stacked MoTe₂/WSe₂ because of the weak interlayer tunneling in the moiré bilayer and the long moiré period (5 nm) that forbids valley mixing for optical transitions. This assumption is supported by the similar optical response for the moiré bilayer and for monolayer TMDs (Supplemental Material, Fig. 2), which is in contrast to the strong moiré exciton resonances observed in other TMD moiré bilayers [40].

III. QAH EFFECT AND TOPOLOGICAL PHASE TRANSITION

We investigate dual-gated devices of AB-stacked MoTe₂/WSe₂ moiré bilayers with doping density of one hole per moiré unit cell at 1.6 K unless otherwise specified. Details on the device fabrication and measurements are provided in Supplemental Material [39]. Figure 2(a) (left) shows the transport data at $E \approx 0.693$ V/nm that support the QAH effect. Particularly, under zero magnetic field the Hall resistance R_{xy} is nearly quantized at the value of h/e^2 (h and e denoting the Planck's constant and elementary charge, respectively), and the longitudinal resistance R_{xx} is

negligible. Both R_{xx} and R_{xy} display a hysteretic magnetic-field dependence with a small coercive field.

Figure 2(b) (middle) is the corresponding helicity-resolved optical reflectance contrast (RC) spectrum under zero magnetic field. The top panel shows the RC for a charge neutral device as a reference. The low- and high-energy spectra are dominated by the response of MoTe₂ and WSe₂, respectively. In the QAH state, RC is dominated by polarons in both layers, including the attractive and repulsive polarons that are redshifted and blueshifted, respectively, from the neutral excitons (the weak repulsive polaron in the heavily hole-doped MoTe₂ is outside the detector range). This indicates that both layers are hole doped. In addition, there is spontaneous spin-valley polarization with nonzero MCD in both layers. The MCD spectrum (bottom panel) is defined as $(I^- - I^+) / (I^- + I^+)$, where I^- and I^+ denote the reflection intensity of the σ^- and σ^+ light, respectively. Here, the sign and spectral line shape are both influenced by the multilayer interference effect in the device (see Supplemental Material [39]). We use the maximum MCD of the attractive polaron feature (averaged over the narrow shaded spectral window) to characterize the spin-valley polarization in each layer [WSe₂ shown in the right-hand panel of Fig. 2(a)]. Figure 2(a) shows that the quantized Hall resistance and the spontaneous spin-valley polarization are correlated.

The correlation between the QAH effect and the spontaneous spin-valley polarization is also supported by the electric-field dependence of the transport and optical properties under zero magnetic field [Fig. 2(c)]. When the electric field exceeds a critical value, $E_c \approx 0.687$ V/nm (dashed line), R_{xx} drops by orders of magnitude to about 1 k Ω , and concurrently, R_{xy} increases from zero to near h/e^2 [Fig. 2(c), top panel]. This is fully consistent with a recent study that reports an electric-field-tuned topological quantum phase transition from a Mott insulator to a QAH insulator [26]. Correlated, the spontaneous spin-valley polarization of each layer increases from zero to a finite value at E_c , but unlike R_{xy} , it does not exhibit a plateau [Fig. 2(c), middle panel]. With further increase of E , R_{xy} and the spontaneous polarization in both layers decrease, signaling a departure from the QAH state.

The layer-resolved RC can also probe the charge distribution in the bilayer [Fig. 2(c), bottom panel]. At small E , the helicity-unresolved RC spectrum of the WSe₂ layer is dominated by a single neutral exciton resonance, indicating a charge neutral layer; at large E , the spectrum consists of two polaron resonances, indicating a doped layer. The transition, determined from the emergence of the polarons, also occurs at E_c . In contrast, the MoTe₂ layer is doped for the entire electric-field range (Supplemental Material, Fig. 3 [39]). The correlation between the emergence of the QAH state and onset of charge transfer from the MoTe₂ layer to the WSe₂ layer further supports the picture that for $E < E_c$ holes reside in

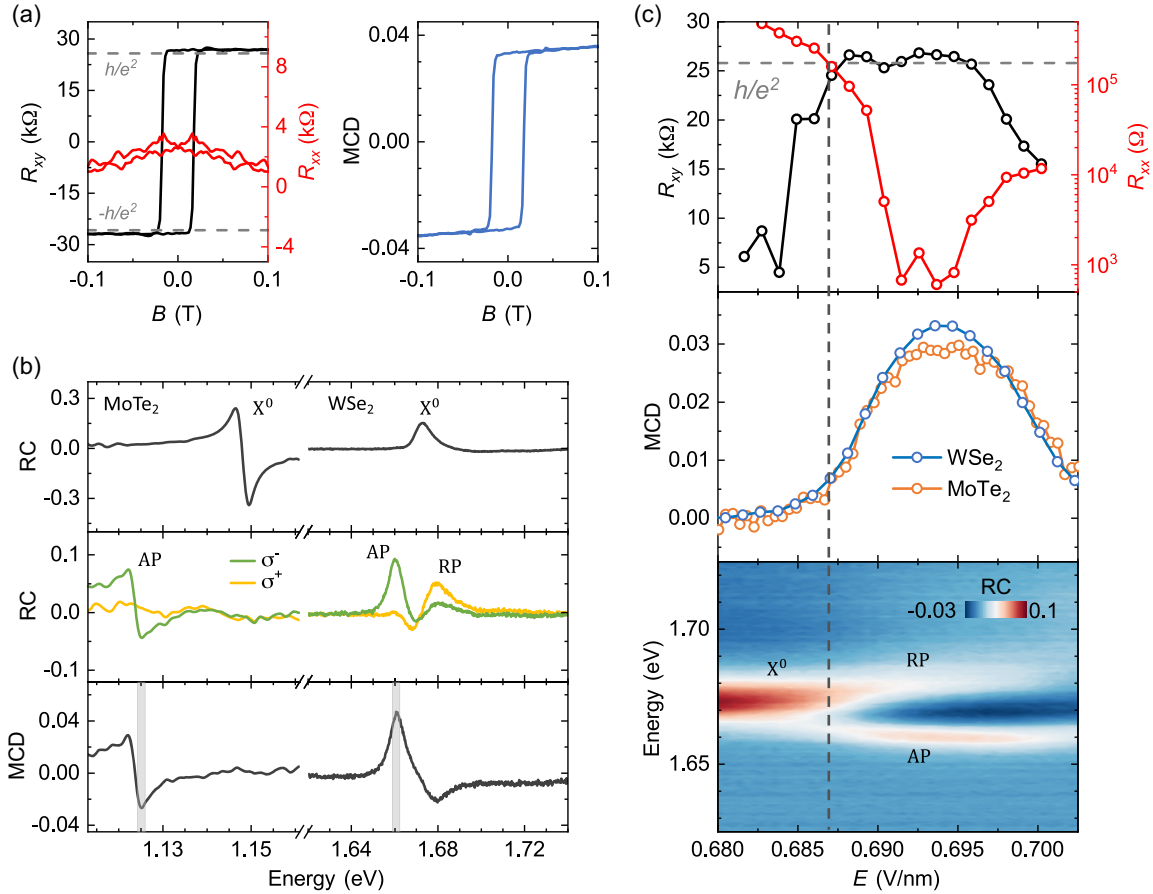


FIG. 2. QAH effect and topological quantum phase transition at 1.6 K. (a) Hysteretic magnetic field dependence of R_{xx} , R_{xy} (left) and MCD in WSe_2 (right) with fixed $E \approx 0.693$ V/nm and doping density of one hole per moiré unit cell. Quantized R_{xy} at the value of h/e^2 (dashed lines) and vanishing R_{xx} at zero magnetic field support the QAH effect. (b) Helicity-resolved reflectance contrast (RC) spectrum of the device in the charge neutral state (top) and the QAH state under zero magnetic field (middle). The two helicities are degenerate in the charge neutral state. The MCD spectrum (bottom) is extracted from the data in the QAH state. The low- and high-energy spectra are dominated by MoTe_2 and WSe_2 , respectively. X^0 , AP, RP denote the neutral exciton, attractive and repulsive polarons, respectively. (c) Electric-field dependence of R_{xy} , R_{xx} (top), absolute MCD in two layers (middle), and RC spectrum of WSe_2 (bottom), all under zero magnetic field. Vertical dashed line denotes the critical field $E_c \approx 0.687$ V/nm for the topological transition from a Mott insulator to a QAH insulator. It also marks the onset of charge transfer from MoTe_2 to WSe_2 .

MoTe_2 and the system is a Mott insulator, and for $E > E_c$ the QAH state arises from electric-field-tuned band inversion and mixing [27,28].

IV. SPONTANEOUS POLARIZATION ALIGNMENT

Next we examine the relative alignment of the spontaneous spin (valley) polarization in the bilayer in the QAH state. Figure 3(a) exhibits the magnetic-field dependence of the helicity-resolved reflection contrast RC^- (top) and RC^+ (bottom). Figure 3(b) is the MCD spectrum extracted from Fig. 3(a). It shows an abrupt sign change near zero field. Magnetic hysteresis can be observed in MCD for a small field range (Supplemental Material, Fig. 4 [39]). In Fig. 3(a), the electric field (≈ 0.693 V/nm) was chosen from the middle of the QAH phase, the magnetic field B

was swept from -8 to 8 T, and the two helicity-resolved spectra were measured together at each B . In addition, since the QAH state disperses in density and magnetic field following the Streda relation [26], we tune the doping density for each field accordingly in order to remain in the QAH state.

A line cut of Figs. 3(a) and 3(b) at $B = 0$ (in backward scan) is displayed in Fig. 2(b). In both layers, the attractive polaron responds mostly to the σ^- excitation. (The repulsive polaron in WSe_2 responds mostly to the σ^+ excitation; this is consistent with the reported opposite optical selection rules for two polaron branches [36,38].) Following the optical selection rules discussed above, the spontaneous spin (valley) polarization is aligned (antialigned) in two layers [Fig. 1(e)]. The assignment is further supported by the nearly identical magnetic-field dependence in two layers. The attractive polaron responds mostly to the

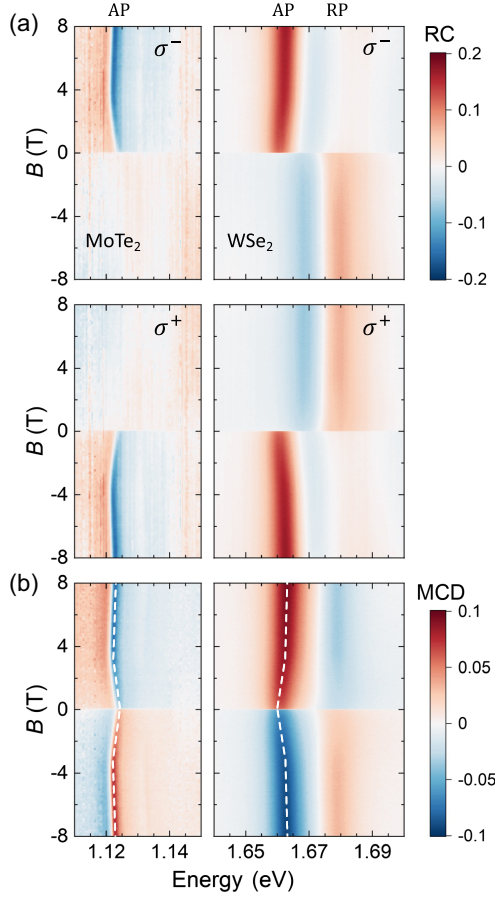


FIG. 3. Spontaneous spin alignment in the bilayer. (a) Magnetic-field dependence of the right-handed (σ^- , top) and left-handed (σ^+ , bottom) reflectance contrast spectrum of MoTe₂ (left) and WSe₂ (right) of the bilayer in the QAH state at 1.6 K. The electric field is fixed at 0.693 V/nm. The two helicity-resolved spectra were measured together at each magnetic field while it was scanned from -8 to 8 T. The doping density was adjusted at each field following the Streda relation to stay in the QAH state. The two layers have nearly identical magnetic-field dependence. (b) Magnetic-field dependent MCD spectra for MoTe₂ (left) and WSe₂ (right) extracted from the data in (a). The white dashed lines denote the maximum (absolute) value of the MCD in each layer.

σ^+ excitation for $B < 0$ T [Fig. 3(a), bottom panel] and to the σ^- excitation for $B > 0$ [Fig. 3(a), top panel]; except for an abrupt change around $B = 0$, the attractive polaron response varies monotonically with field and saturates at high fields. Note that the magnetic field aligns both the spin and orbital magnetic moments in each layer; the two contributions have the same sign as in monolayer TMDs [25] although the layers are AB stacked. Also note that if the spontaneous spin polarization were antialigned [Fig. 1(d)], the attractive polarons would appear at different helicity channels at a given magnetic field (Supplemental Material, Fig. 5 [39]), and a switch of the excitation helicity

for one of the layers would be expected before magnetic saturation, where all spins should be aligned; both are in contradiction to our experimental observation.

V. SIGNATURE OF A CANTED SPIN TEXTURE

We summarize the magnetic-field dependence of the out-of-plane spin polarization by following the maximum MCD of the attractive polaron feature in each layer [Fig. 4(a)]. The low-field behavior including the magnetic hysteresis is included as an inset. Although the MCD sign is influenced by the multilayer interference effect, the attractive polaron oscillator strength for each helicity is not [see Fig. 3(a) and Supplemental Material [39]]; we thus set MCD in both layers to be positive for $B > 0$, where the spin polarization in two layers is aligned. For comparison, we also normalize MCD in each layer to its saturated value at 8 T. Beyond the hysteresis loop, MCD increases monotonically with magnetic field in both layers [Fig. 4(a)]. In WSe₂, it saturates near 6 T, and the zero-field MCD is about 60% of the saturation value. In MoTe₂, MCD saturates near 8 T, and the zero-field value is about 45% of the saturation value. This behavior is qualitatively different from that of R_{xy} , which is quantized at zero field and does not depend on the magnetic field. Our result shows that full spin polarization is not required for quantized Hall transport; this is also consistent with the absence of an MCD plateau even when there is a quantized R_{xy} plateau in Fig. 2(c).

We also perform temperature dependence study of MCD in Fig. 4(b) to elucidate the role of thermal fluctuations. All curves are normalized by the MCD value at 8 T and 1.6 K in each layer (i.e., magnetic saturation). As temperature T increases, the spontaneous MCD weakens, but the slow magnetic saturation beyond the hysteresis loop remains nearly unchanged. Figure 4(c) (top) displays the temperature dependence of the spontaneous MCD (the spectra are included in Supplemental Material Fig. 6 [39]). It decreases monotonically with increasing temperature; for $T \leq 2$ K, the change is small, indicating saturated spontaneous polarization. Above the magnetic ordering temperature ($5\text{--}6$ K), the spontaneous MCD decreases to zero. We can also extract the slope of the magnetic-field dependence of MCD at zero field, which is proportional to the spin or magnetic susceptibility χ [41]. The temperature dependence of χ is well described by the Curie-Weiss law, $\chi^{-1} \propto T - \theta$, with Curie-Weiss temperature $\theta \approx 5$ K [dashed line in Fig. 4(c) bottom panel]. The value reflects the energy scale of the ferromagnetic interaction between the local moments in the QAH insulator. Thermal fluctuations at 1.6 K are thus unimportant. Our result supports canted spin with nonzero in-plane component in the QAH state.

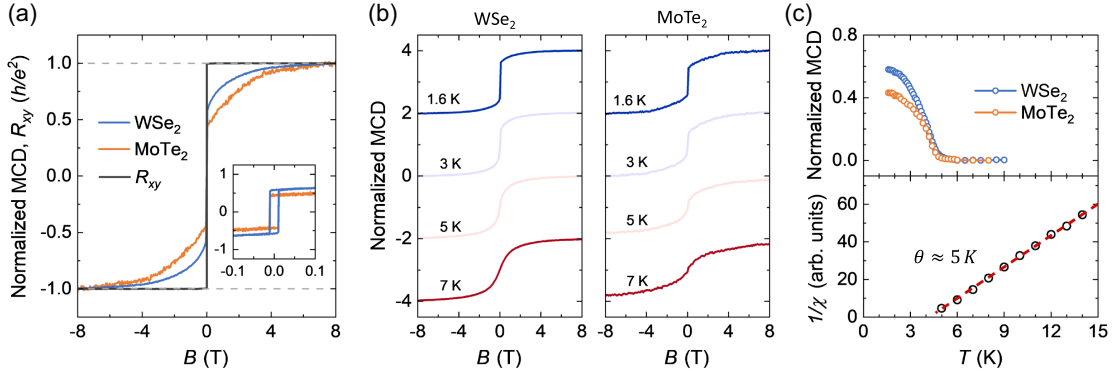


FIG. 4. Signature of a canted spin texture. (a) Magnetic-field dependence of normalized MCD in each layer in the range of ± 8 and ± 0.1 T (inset) at 1.6 K. The MCD is averaged over a narrow spectral range of 0.9 meV centered at the maximum of the attractive polaron feature [dashed lines in Fig. 3(b)]. It is normalized by the value at 8 T in each layer. The MCD shows an abrupt change near zero field and saturates slowly with increasing field. In contrast, R_{xy} (right-hand axis) is quantized at the value of h/e^2 (dashed lines) near zero magnetic field and does not depend on field. (b) Same as (a) at varying temperatures. All curves are normalized by MCD at 8 T and 1.6 K in each layer. The curves are vertically displaced for clarity. (c) Temperature dependence of the spontaneous MCD for MoTe₂ and WSe₂ (top). Both saturate below 2 K and vanish above 5–6 K. Bottom: temperature dependence of the spin (or magnetic) susceptibility in WSe₂ (symbols) above the magnetic ordering temperature. It is well described by the Curie-Weiss law, $\chi^{-1} \propto T - \theta$, with a Curie-Weiss temperature $\theta \approx 5$ K (red line).

VI. DISCUSSION

The observed spin-polarized QAH ground state with canted spin textures is unexpected. [Note that the canted spin texture is not illustrated in Fig. 1(e).] The current theoretical studies without considering the spin-dependent interactions have shown that the valley-polarized state is the stable ground state [Fig. 1(d)], i.e., hybridization of states from different layers but from the same valley near the Fermi level [27–32]. The spin-polarized QAH state requires mixing states from different layers and different valleys; a correlated charge gap is opened at the Fermi level; the state is thus spontaneous layer and valley coherent [33,34]. Such a state could occur, for instance, via an exciton condensation mechanism near band inversion [33,34], which is favored by the weak interlayer coupling in AB-stacked TMD bilayers [32–34]. Future experiments with an ultrathin spacer between the TMD bilayers that quenches the interlayer tunneling while maintaining the strong Coulomb interaction and reasonable moiré potential could test the validity of the mechanism.

The origin of the observed canted spin texture for the QAH state is also not understood. One possible explanation comes from the close proximity of the QAH insulator to a 120° Néel-ordered Mott insulator (an intralayer- and intervalley-coherent state) and the possibility of inheriting the noncollinear spin configuration [28]. The weaker spontaneous MCD and higher saturation magnetic field in MoTe₂ could be related to the weaker Ising spin-orbit coupling in MoTe₂. Another possibility is the Rashba spin-orbit coupling, which becomes important under high out-of-plane electric fields and can cause spin canting. Our results call for a better understanding of the microscopic

origin of the QAH state and its magnetic ground state in AB-stacked MoTe₂/WSe₂ moiré bilayers.

ACKNOWLEDGMENTS

We thank Yang Zhang, Trithip Devakul, Liang Fu, Yongxin Zeng, Nemin Wei, Allan MacDonald, Ming Xie, K. T. Law, Ya-Hui Zhang, and Feng Wang for many insightful discussions. This work was supported by the U.S. Department of Energy, Office of Science, Basic Energy Sciences, under Awards No. DE-SC0019481 at Cornell and No. FWP-100459 at SLAC (optical measurements), the Air Force Office of Scientific Research under Grant No. FA9550-19-1-0390 (sample and device fabrication), and the National Science Foundation under Grant No. DMR-1807810 (transport measurements). The growth of the *h*-BN crystals was supported by the Elemental Strategy Initiative of MEXT, Japan, and CREST (JPMJCR15F3), JST. The work was also funded in part by the Gordon and Betty Moore Foundation through Grant No. GBMF11563 and through the EPiQS Initiative through Grant No. GBMF9462. Device fabrication made use of the Cornell NanoScale Facility, an NNCI member supported by NSF Grant No. NNCI-2025233.

- [1] E. Y. Andrei and A. H. MacDonald, *Graphene bilayers with a twist*, *Nat. Mater.* **19**, 1265 (2020).
- [2] J. Liu and X. Dai, *Orbital magnetic states in moiré graphene systems*, *Nat. Rev. Phys.* **3**, 367 (2021).
- [3] W. Witczak-Krempa, G. Chen, Y. B. Kim, and L. Balents, *Correlated quantum phenomena in the strong spin-orbit regime*, *Annu. Rev. Condens. Matter Phys.* **5**, 57 (2014).

- [4] L. Balents, C. R. Dean, D. K. Efetov, and A. F. Young, *Superconductivity and strong correlations in moiré flat bands*, *Nat. Phys.* **16**, 725 (2020).
- [5] D. M. Kennes, M. Claassen, L. Xian, A. Georges, A. J. Millis, J. Hone, C. R. Dean, D. N. Basov, A. N. Pasupathy, and A. Rubio, *Moiré heterostructures as a condensed-matter quantum simulator*, *Nat. Phys.* **17**, 155 (2021).
- [6] K. F. Mak and J. Shan, *Semiconductor moiré materials*, *Nat. Nanotechnol.* **17**, 686 (2022).
- [7] Y. Cao, V. Fatemi, S. Fang, K. Watanabe, T. Taniguchi, E. Kaxiras, and P. Jarillo-Herrero, *Unconventional superconductivity in magic-angle graphene superlattices*, *Nature (London)* **556**, 43 (2018).
- [8] Y.-H. Zhang, D. Mao, Y. Cao, P. Jarillo-Herrero, and T. Senthil, *Nearly flat Chern bands in moiré superlattices*, *Phys. Rev. B* **99**, 075127 (2019).
- [9] F. Wu, T. Lovorn, E. Tutuc, I. Martin, and A. H. MacDonald, *Topological insulators in twisted transition metal dichalcogenide homobilayers*, *Phys. Rev. Lett.* **122**, 086402 (2019).
- [10] N. Bultinck, S. Chatterjee, and M. P. Zaletel, *Mechanism for anomalous Hall ferromagnetism in twisted bilayer graphene*, *Phys. Rev. Lett.* **124**, 166601 (2020).
- [11] F. Wu and S. Das Sarma, *Collective excitations of quantum anomalous Hall ferromagnets in twisted bilayer graphene*, *Phys. Rev. Lett.* **124**, 046403 (2020).
- [12] C. Repellin, Z. Dong, Y.-H. Zhang, and T. Senthil, *Ferromagnetism in narrow bands of moiré superlattices*, *Phys. Rev. Lett.* **124**, 187601 (2020).
- [13] T. Li, J. Zhu, Y. Tang, K. Watanabe, T. Taniguchi, V. Elser, J. Shan, and K. F. Mak, *Charge-order-enhanced capacitance in semiconductor moiré superlattices*, *Nat. Nanotechnol.* **16**, 1068 (2021).
- [14] C.-Z. Chang, J. Zhang, X. Feng, J. Shen, Z. Zhang, M. Guo, K. Li, Y. Ou, P. Wei, L.-L. Wang *et al.*, *Experimental observation of the quantum anomalous Hall effect in a magnetic topological insulator*, *Science* **340**, 167 (2013).
- [15] X. Kou, S.-T. Guo, Y. Fan, L. Pan, M. Lang, Y. Jiang, Q. Shao, T. Nie, K. Murata, J. Tang, Y. Wang, L. He, T.-K. Lee, W.-L. Lee, and K. L. Wang, *Scale-invariant quantum anomalous Hall effect in magnetic topological insulators beyond the two-dimensional limit*, *Phys. Rev. Lett.* **113**, 137201 (2014).
- [16] C.-X. Liu, S.-C. Zhang, and X.-L. Qi, *The quantum anomalous Hall effect: Theory and experiment*, *Annu. Rev. Condens. Matter Phys.* **7**, 301 (2016).
- [17] A. L. Sharpe, E. J. Fox, A. W. Barnard, J. Finney, K. Watanabe, T. Taniguchi, M. A. Kastner, and D. Goldhaber-Gordon, *Emergent ferromagnetism near three-quarters filling in twisted bilayer graphene*, *Science* **365**, 605 (2019).
- [18] G. Chen, A. L. Sharpe, E. J. Fox, Y.-H. Zhang, S. Wang, L. Jiang, B. Lyu, H. Li, K. Watanabe, T. Taniguchi, Z. Shi, T. Senthil, D. Goldhaber-Gordon, Y. Zhang, and F. Wang, *Tunable correlated Chern insulator and ferromagnetism in a moiré superlattice*, *Nature (London)* **579**, 56 (2020).
- [19] M. Serlin, C. L. Tschirhart, H. Polshyn, Y. Zhang, J. Zhu, K. Watanabe, T. Taniguchi, L. Balents, and A. F. Young, *Intrinsic quantized anomalous Hall effect in a moiré heterostructure*, *Science* **367**, 900 (2020).
- [20] H. Polshyn, J. Zhu, M. A. Kumar, Y. Zhang, F. Yang, C. L. Tschirhart, M. Serlin, K. Watanabe, T. Taniguchi, A. H. MacDonald, and A. F. Young, *Electrical switching of magnetic order in an orbital Chern insulator*, *Nature (London)* **588**, 66 (2020).
- [21] T. Li, S. Jiang, L. Li, Y. Zhang, K. Kang, J. Zhu, K. Watanabe, T. Taniguchi, D. Chowdhury, and L. Fu, J. Shan, and K. F. Mak, *Continuous Mott transition in semiconductor moiré superlattices*, *Nature (London)* **597**, 350 (2021).
- [22] H. Polshyn, Y. Zhang, M. A. Kumar, T. Soejima, P. Ledwith, K. Watanabe, T. Taniguchi, A. Vishwanath, M. P. Zaletel, and A. F. Young, *Topological charge density waves at half-integer filling of a moiré superlattice*, *Nat. Phys.* **18**, 42 (2022).
- [23] T. Devakul, V. Crépel, Y. Zhang, and L. Fu, *Magic in twisted transition metal dichalcogenide bilayers*, *Nat. Commun.* **12**, 6730 (2021).
- [24] X. Xu, W. Yao, D. Xiao, and T. F. Heinz, *Spin and pseudospins in layered transition metal dichalcogenides*, *Nat. Phys.* **10**, 343 (2014).
- [25] K. F. Mak, D. Xiao, and J. Shan, *Light-valley interactions in 2D semiconductors*, *Nat. Photonics* **12**, 451 (2018).
- [26] T. Li, S. Jiang, B. Shen, Y. Zhang, L. Li, Z. Tao, T. Devakul, K. Watanabe, T. Taniguchi, L. Fu, J. Shan, and K. F. Mak, *Quantum anomalous Hall effect from intertwined moiré bands*, *Nature (London)* **600**, 641 (2021).
- [27] Y. Zhang, T. Devakul, and L. Fu, *Spin-textured Chern bands in AB-stacked transition metal dichalcogenide bilayers*, *Proc. Natl. Acad. Sci. U.S.A.* **118**, e2112673118 (2021).
- [28] T. Devakul and L. Fu, *Quantum anomalous Hall effect from inverted charge transfer gap*, *Phys. Rev. X* **12**, 021031 (2022).
- [29] Y.-M. Xie, C.-P. Zhang, J.-X. Hu, K. F. Mak, and K. T. Law, *Valley-polarized quantum anomalous Hall state in moiré MoTe₂/WSe₂ heterobilayers*, *Phys. Rev. Lett.* **128**, 026402 (2022).
- [30] H. Pan, M. Xie, F. Wu, and S. Das Sarma, *Topological phases in AB-stacked MoTe₂/WSe₂ topological insulators, Chern insulators, and topological charge density waves*, *Phys. Rev. Lett.* **129**, 056804 (2022).
- [31] Ming Xie, Haining Pan, Fengcheng Wu, and S. D. Sarma, *Nematic excitonic insulator in transition metal dichalcogenide moiré heterobilayers*, *Phys. Rev. Lett.* **131**, 046402 (2023).
- [32] Yao-Wen Chang and Y.-C. Chang, *Theory of quantum anomalous Hall effect and electric-field-induced phase transition in AB-stacked MoTe₂/WSe₂ moiré heterobilayers*, *Phys. Rev. B* **106**, 245412 (2022).
- [33] Ying-Ming Xie, Cheng-Ping Zhang, and K. T. Law, *Topological $p_x + ip_y$ inter-valley coherent state in moiré MoTe₂/WSe₂ heterobilayers*, [arXiv:2206.11666](https://arxiv.org/abs/2206.11666).
- [34] Zhihuan Dong and Y.-H. Zhang, *Excitonic Chern insulator and kinetic ferromagnetism in MoTe₂/WSe₂ moiré bilayer*, *Phys. Rev. B* **107**, L081101 (2023).
- [35] Y. Su, H. Li, C. Zhang, K. Sun, and S.-Z. Lin, *Massive Dirac fermions in moiré superlattices: A route towards topological flat minibands and correlated topological insulators*, *Phys. Rev. Res.* **4**, L032024 (2022).

- [36] M. Sidler, P. Back, O. Cotlet, A. Srivastava, T. Fink, M. Kroner, E. Demler, and A. Imamoglu, *Fermi polaron-polaritons in charge-tunable atomically thin semiconductors*, *Nat. Phys.* **13**, 255 (2017).
- [37] D. K. Efimkin and A. H. MacDonald, *Many-body theory of trion absorption features in two-dimensional semiconductors*, *Phys. Rev. B* **95**, 035417 (2017).
- [38] T. Wang, Z. Li, Z. Lu, Y. Li, S. Miao, Z. Lian, Y. Meng, M. Blei, T. Taniguchi, K. Watanabe, S. Tongay, W. Yao, D. Smirnov, C. Zhang, and S.-F. Shi, *Observation of quantized exciton energies in monolayer WSe₂ under a strong magnetic field*, *Phys. Rev. X* **10**, 021024 (2020).
- [39] See Supplemental Material at <http://link.aps.org/supplemental/10.1103/PhysRevX.14.011004> for reflection contrast spectra in moiré heterostructure.
- [40] C. Jin, E. C. Regan, A. Yan, M. Iqbal Bakti Utama, D. Wang, S. Zhao, Y. Qin, S. Yang, Z. Zheng, S. Shi, K. Watanabe, T. Taniguchi, S. Tongay, A. Zettl, and F. Wang, *Observation of moiré excitons in WSe₂/WS₂ heterostructure superlattices*, *Nature (London)* **567**, 76 (2019).
- [41] Y. Tang, L. Li, T. Li, Y. Xu, S. Liu, K. Barmak, K. Watanabe, T. Taniguchi, A. H. MacDonald, J. Shan, and K. F. Mak, *Simulation of Hubbard model physics in WSe₂/WS₂ moiré superlattices*, *Nature (London)* **579**, 353 (2020).